Full Paper

Wiley Online Library

ELECTROANALYSIS

DOI: 10.1002/elan.201900199

Determination of Electrochemical Interaction Between 2-(1H-benzimidazol-2-yl) Phenol and DNA Sequences

Seda Nur Topkaya*[a] and Arif E. Cetin[b]

Abstract: A benzimidazole derivate, 2-(1H-benzimidazol-2-yl) phenol (2-Bip) and its interaction mechanism with sequence specific DNA was examined with Differential Pulse Voltammetry (DPV). We, for the first time, investigated the effect of 2-Bip on sequence specific DNA with electrochemical methods by evaluating both guanine and 2-Bip oxidation signal changes. In the study, probe sequences were immobilized to the surface of the electrodes and then hybridization was achieved by sending the complementary target onto the probe modified electrodes. Following the hybridization, 2-Bip solution was interacted with probe and hybrid sequences to see the effect of 2-Bip on different DNA sequences. The binding constant (K), toxicity (S%) and thermodynamic parameters, i.e., Gibbs free energy (ΔG°) of 2-Bip-DNA complexes were evaluated. K was calculated as 5×10^5 and the change in the ΔG° was found as $-32.50\,kJ\,mol^{-1}$, which are consistent well with the literature. Furthermore, S% showed that 2-Bip is moderately toxic to single stranded DNA (ssDNA) and toxic to double stranded DNA (dsDNA). From our experimental data, we made four conclusions (i) 2-Bip affects both ssDNA and dsDNA, (ii) 2-Bip interaction mode with DNA could be non-covalent interactions, (iii) 2-Bip could be used as new DNA hybridization indicator due to its distinct effects on ssDNA and dsDNA, (iv) 2-Bip could be used as a drug molecule for its DNA effect.

Keywords: Electrochemical Biosensor · Drug · 2-(1H-benzimidazol-2-yl) phenol · Hybridization Indicator · Drug-DNA Interaction

1 Introduction

DNA is a key molecule in replication, transcription, protein coding and cell integrity as well as in carrying the genetic information for inheritance and widely used as a primary pharmacological target to investigate the properties of drugs [1]. Studies on interaction of DNA with drugs have been an active field of pharmaceutical research [2]. Revealing of the underlying mechanisms of interaction between DNA and drug molecules is essential for getting information about the rational design of new types of molecules. Thus, it is necessary to understand the binding mode and its relevance to drug activity and toxicity [3].

Small molecules such as drugs, ligands and chemicals can interact with DNA by covalent and non-covalent interactions. Covalent interactions (e.g., cis-platin binding to guanine bases) lead to chemical alterations of DNA that is irreversible and cause cell death. Non-covalent interactions are a class of intermolecular forces, which are relatively weaker than the covalent interactions.

Drug and DNA molecules experience certain modifications such that DNA conformation is mostly reversible for non-covalent interactions, which could be divided into three main groups: electrostatic binding, intercalation and groove binding (major and minor grooves) [4]. Electrostatic binding occurs due to interaction between the negatively charged phosphate backbone of DNA and the positively charged ends of small molecules. Intercalators are molecules that stack perpendicular to double stranded (dsDNA) structures through different modes such as Van der Waals, hydrogen bonding or hydrophobic interactions that form a stable DNA-intercalator complex. Another non-covalent interaction mode, groove binding, involves hydrogen bonding or Van der Waals interactions of small molecule with nucleic acid bases through intermolecular forces in a sequence either dependent or independent modes. The most biologically found form of DNA is the B-form that has a characteristic wide-deep major groove and narrow-deep minor groove, where the latter is with a higher negative density charge. Intercalation and groove binding are two most typical modes by which small molecules bind directly and selectively to dsDNA. As a sub-group of non-covalent interactions, London dispersion forces are found in all molecules. London dispersion forces are the weakest type of non-covalent interaction. They are also known as "induced dipole-induced dipole interactions" and present between all molecules, even the ones that inherently do not have permanent dipoles.

DNA and small molecules' interaction can be monitored with many techniques such as molecular modeling [2f,5], foot-printing [6], Nuclear Magnetic Resonance

[a] S. N. Topkaya
Department of Analytical Chemistry, Faculty of Pharmacy, Izmir Katip Celebi University, 35620, Cigli, Izmir, TURKEY
Phone: +90 232 329 35 35-6140
E-mail: sedanur6@gmail.com
sedanur.topkaya@ikc.edu.tr
[b] A. E. Cetin
Izmir Biomedicine and Genome Center, Izmir, TURKEY

(NMR) [7], Mass Spectrometry (MS) [8], FTIR [9] and Raman Spectroscopy [10], Capillary Electrophoresis [11] and Surface Plasmon Resonance (SPR) [12]. Spectroscopic techniques are also widely used to monitor drug-nucleic acid interactions such as UV-Vis [13], fluorescence [14] and colorimetry [15].

To explore interaction mechanisms between drugs or drug candidates, electrochemical methods can provide useful information about binding constants and site size in a rapid, easy and sensitive manner compared to techniques explained above [16].

Benzimidazoles, heterocyclic and aromatic compounds, are formed by the fusion of the benzene and imidazole ring system. Benzimidazoles could be modified by adding substituents on different positions of main ring structure and these modifications can cause notable changes in the electronic, steric and hydrophobic properties of the compounds. Benzimidazoles are structurally similar to purine bases and they can interact with natural macromolecules such as proteins, enzymes and nucleic acids [17]. Benzimidazoles and their derivates that differ in their chemical and physical properties based on type and position of functional groups have been extensively studied for their antioxidant, antimicrobial, anticoagulant and antihypertensive properties [18]. In addition, it has been also suggested that benzimidazoles are the most featured heterocycle that have favorable cytotoxic properties against different types of cancer cell lines [19]. For instance, 2-substituted benzimidazoles with -chloro or -carboxyl group at 5-position are reported as potent anticancer agents [20]. In addition, pyrimidine [21], pyrazoline [22] and thiazole [23] derivatives have been extensively investigated for their anticancer effect. Especially, bis-benzimidazoles (Hoechst-33342 and Hoechst-33258) are another very important class of benzimidazole derivates that show DNA topoisomerase I inhibitory activities.

In this article, we, for the first time, examined electrochemical properties of a benzimidazole derivate, 2-(1H-benzimidazol-2-yl) phenol (2-Bip), and its interaction mechanism with sequence specific DNA with Differential Pulse Voltammetry (DPV). There has been no literature for 2-Bip in connection with single (ssDNA) and double (dsDNA) stranded DNA's with voltammetric techniques.

Our study is the first to investigate the effect of 2-Bip on the sequence specific DNA with electrochemical methods. As drugs show their pharmacological activities with different mechanisms, it is extremely important to understand the underlying mechanism of their interaction with DNA, e.g., 2-Bip, a potential drug.

First, redox properties of 2-Bip were analyzed, and then numerous factors affecting probe immobilization, target hybridization and drug interaction were optimized. Our findings were very promising in terms of 2-Bip binding to ssDNA or dsDNA, that caused notable changes in current compared to before interaction with DNA, which clearly demonstrated the effect of 2-Bip on DNA sequences. Upon the interaction with 2-Bip, guanine oxidation signals decreased dramatically. The signal differences enabled us to distinguish between ssDNA and dsDNA without using labels by simply analyzing oxidation signals of DNA guanine bases at approximately 1.0 V vs. Ag/AgCl. Moreover, 2-Bip oxidation signal was observed at 0.75 V and 2-Bip gives distinct oxidation signals when interacted with ssDNA and dsDNA, i.e., it can be used as a new DNA hybridization indicator. Consequently, 2-Bip interaction mode with DNA could be non-covalent interaction, and 2-Bip could be a potential drug molecule thanks to its DNA effect.

2 Experimental

2.1 Instruments

Voltammetric measurements were performed with AUTOLAB-PGSTAT 30 electrochemical analysis system. The three-electrode system is consisted of a Pencil Graphite Electrode (PGE) functioning as the working electrode, a reference electrode (Ag/AgCl) and a platinum wire working as the auxiliary electrode.

2.2 Chemicals

1-Ethyl-3-(3-dimethylaminopropyl)carbodiimide hydrochloride (EDC), N-hydroxysuccinimide (NHS), 2-(1H- benzimidazole-2-yl)phenol and other chemicals were used (Sigma Aldrich).

2.3 2-(1H-benzimidazol-2-yl) Phenol

2-Bip was dissolved in Dimethyl sulfoxide (DMSO). Diluted 2-Bip concentrations were prepared in 0.05 M phosphate buffer (20 mM NaCl, PBS; pH 7.4). Chemical structure of 2-(1H-benzimidazol-2-yl) phenol is shown in Figure 1.

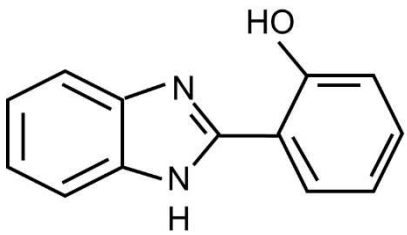

Fig. 1. Chemical structure of 2-(1H-benzimidazol-2-yl) phenol.

2.4 Oligonucleotides

HPLC grade DNA oligonucleotides were prepared by dissolving DNA in three-distilled water. Dilute probe solutions were prepared in 0.05 M acetate buffer solution (ACB; pH 4.8) containing 20 mM NaCl. Diluted target solutions were prepared in 0.5 M phosphate buffer

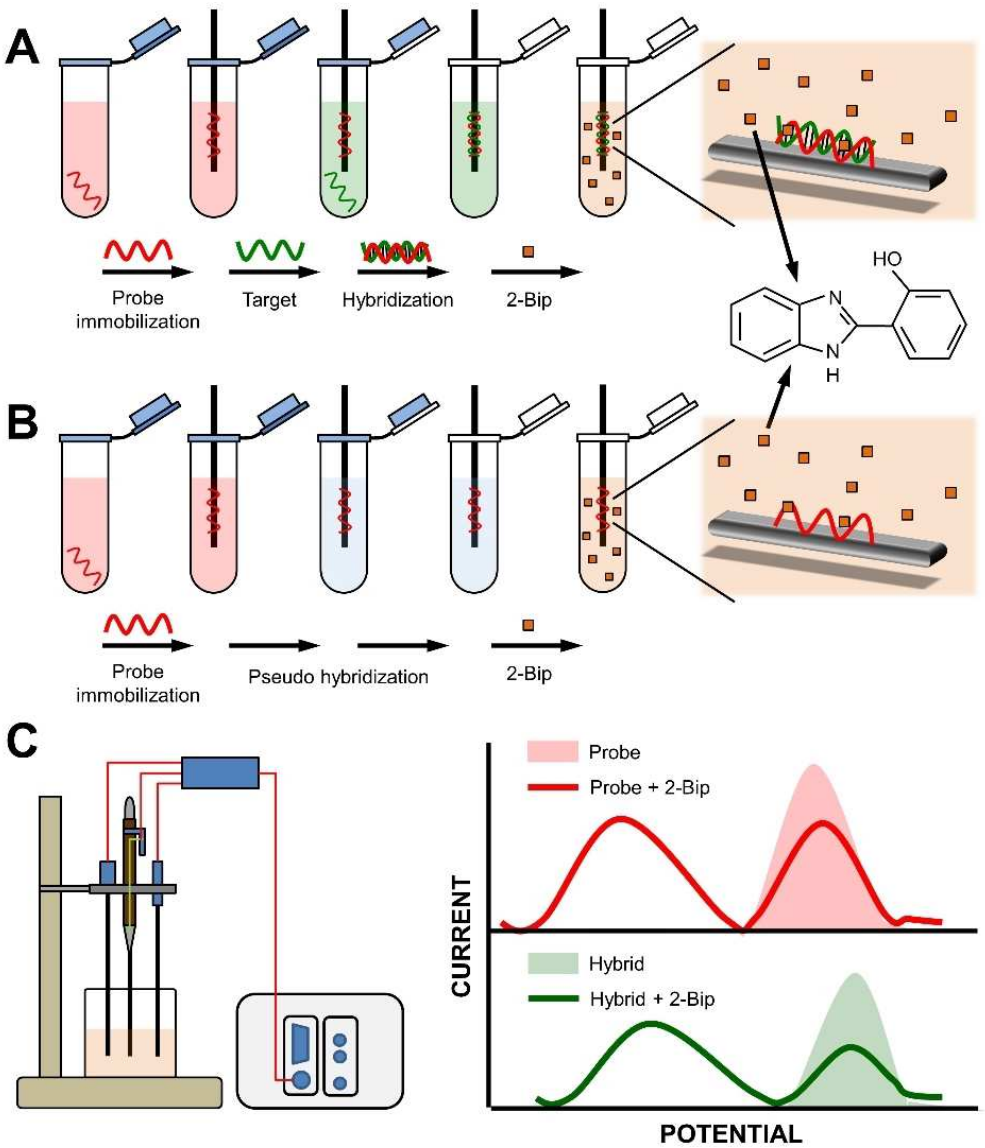

Scheme 1. Experimental steps: 2-Bip interaction with (A) dsDNA and (B) ssDNA. Conditions: Probe modified PGEs were immersed into (A) target solution and (B) PBS for 30 min, and later interacted with 2-Bip. (C) DPV measurement by scanning between 0.55 V and 1.15 V in PBS.

solution (PBS; 7.4) containing 20 mM NaCl. 0.1 M tris buffer solutions (TBS; pH 8.0) containing 20 mM NaCl were also used.

The probe length was chosen as 20 bases since long probes (more than 30 bases) require longer hybridization duration and causes slow synthesis, while shorter probes (less than 15 bases) are lack of specificity. DNA base sequences were chosen as below:

Probe – 5′-TTC GGG GTG TAG CGG TCG TC-3′ – 65% GC Content

Target – 5′-GAC GAC CGC TAC ACC CCG AA-3′ – 65% GC Content

Control – 5′-ACC TTC GGC AAA AGC TTC AAT ACT CCA3′ – 44% GC Content

2.5 Procedure

The experimental procedure (Scheme 1) for electrochemical detection of DNA interaction with 2-Bip was composed of following steps:

(i) Pre-treatment of electrodes: PGEs were pre-treated by applying 1.4 V for 30 sec. in ACB to create –COOH groups to enhance the adsorptive accumulation of DNA oligonucleotides [24].

(ii) Immobilization of probe sequence onto electrode surface: Three different immobilization methods were tested to find the best probe immobilization method:

- **Adsorption**: Pretreated PGEs were immersed into 5 μg/mL DNA probe solution for 20 min. After probe immobilization, PGEs were rinsed with ACB.
- **Electrostatic attraction**: ssDNA was immobilized on pretreated PGEs by applying +0.50 V potential for 5 min in 5 μg/mL dsDNA solution with 200 rpm stirring. The electrodes were then rinsed with ACB.
- **Covalent attachment**: Electrodes were immersed into 2 mM EDC and 5 mM NHS solution for 1 h. to achieve covalent surface activation. Then, PGEs were washed in PBS and immersed in 5 μg/mL DNA for 20 min. After probe immobilization, PGEs were rinsed with ACB.

(iii) Hybridization between probe and target sequences: Probe modified PGEs were dipped into 7 μg/mL target for 20 min. Electrodes were rinsed with PBS. The same procedure was also performed with control sequence instead of target oligonucleotide.

(iv) DNA oligonucleotide interaction with 2-Bip: After coating of the electrodes with probe and hybrid DNA, 15 μg/mL of 2-Bip was interacted with DNA modified electrodes for 7 min. Then, electrodes were rinsed with PBS.

(v) Measurement: DPV was used to measure the changes in guanine oxidation signals and before and after the 2-Bip for potential ranges from 0.55 V to 1.15 V (step potential: 8 mV, modulation amplitude: 80 mV, scan rate: 50 mV/s).

3 Results and Discussion

In order to understand the interaction mechanism between drug molecules and DNA, electrochemical responses of DNA before and after the interaction with drugs can be used, i. e.,

- A dramatic decrease/increase at the oxidation/reduction peak current of **the drug** which selectively binds to ssDNA or dsDNA,
- A dramatic decrease/increase at oxidation/reduction peak current of **the electroactive DNA bases** such as guanine or adenine,
- Potential shifts to the more positive or negative side by the intercalation of nucleic acid-binding molecules into ssDNA or dsDNA.

In this study, we evaluated all these signals explained above.

In, a voltammogram is shown for the oxidation of 2-Bip and guanine bases in the same measurement window by scanning from 0.55 V to 1.15 V to see the effect of pH on interaction efficiency in ACB, PBS and TBS.

As shown in Figure 2, 2-Bip oxidation signal was nearly at 0.75 V–0.8 V, whereas guanine signal was at 1.0 V. 2-Bip measured in different pH values showed only one anodic peak corresponding to the direct oxidation of amino to nitro groups. The oxidation potential of 2-Bip shifted to lower potentials with the increase in pH, indicating that the electrochemical oxidation of 2-Bip was associated with a proton-transfer process. The highest 2-

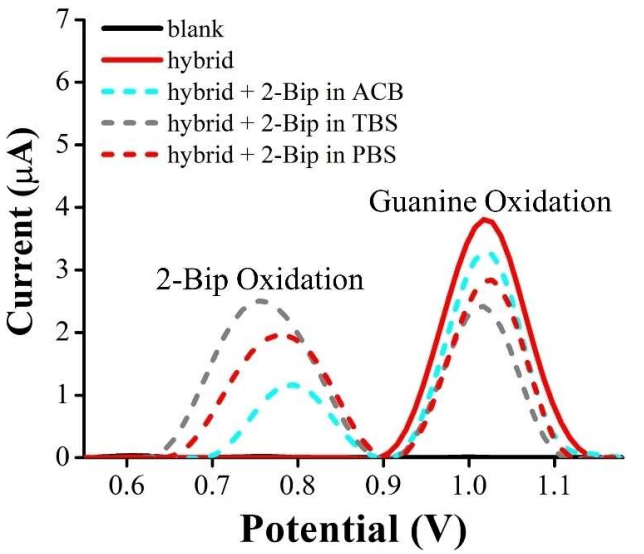

Fig. 2. Voltammogram of oxidation signals of 2-Bip (0.75 V–0.8 V) and guanine (1.0 V) measured for blank (bare electrode measured in ACB), 2-Bip, hybrid, and hybrid + 2-Bip coated PGEs measured with DPV in ACB (pH: 4.8), PBS (pH: 7.4) and TBS (pH: 8.0).

Bip oxidation signals were recorded at a basic pH value, which is TBS. On the other hand, remarkable shifts for the oxidation signal of guanine after the interaction with 2-Bip were not observed. As opposed to 2-Bip for guanine, the current magnitudes decrease with pH. This can be related to low electrostatic repulsion at basic pH. As the signals of 2-Bip and guanine were moderate in PBS (close to physiological pH level), the voltammetric measurements throughout the article were performed in PBS.

Figure 3A and 3B show the calibration studies for the electrochemical response. Figure 3A shows the voltammogram of 2-Bip and guanine oxidation signals as a function of interaction time from 0 to 10 min. As shown in Figure 3A, the peak currents of guanine decreased with interaction time. In contrast, the 2-Bip oxidation signal increased with time due to accumulation and remained nearly unchanged after 7 min. Thus, 7 min was chosen as the optimum interaction time for forthcoming studies.

The effect of 2-Bip concentration on biosensor response was studied for 0 to 10 μg/mL (Figure 3B). Increasing 2-Bip concentration caused a decrease in the oxidation peak current of guanine, which corresponds to 2-Bip binding to guanine. The lowest guanine signal was obtained for 10 μg/mL. On the other hand, there was a gradual increase of current with 2-Bip concentration. Maximum decrease at guanine signal and increase at drug signal was recorded at 10 μg/mL of 2-Bip. Therefore, 15 μg/mL was chosen as the optimum concentration for 2-Bip.

Immobilization of DNA probe onto surface of the electrodes to recognize its complementary target via hybridization is the most important step in the construc-

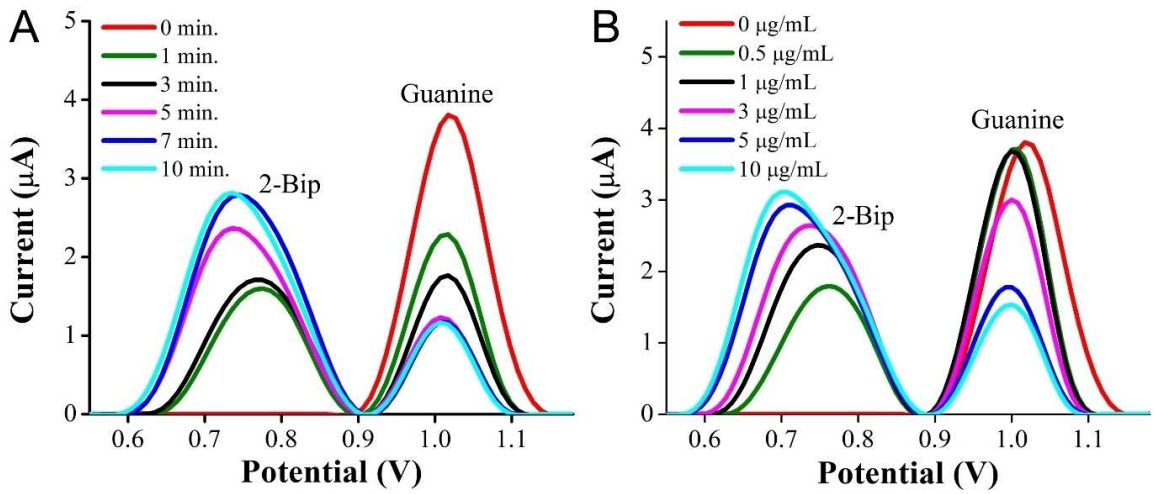

Fig. 3. Voltammogram of oxidation signals for 2-Bip (0.75 V) and guanine (1.0 V) measured from 2-Bip and hybrid + 2-Bip coated PGEs at (A) different interaction times ranging from 0 to10 min., and (B) different concentrations of 2-Bip ranging from 0 to 15 μg/mL. The corresponding experimental procedure: PGEs pretreatment in ACB, 5 μg/mL probe immobilization, interaction with 7 μg/mL target for 30 min, rinsing with PBS, interaction with 2-Bip for different conditions and DPV measurement by scanning between 0.55 V and 1.15 V in PBS.

tion of biosensor. It is crucial to select the optimum method to ensure the immobilized DNA probes that are strongly stabilized on the working electrode surface without desorption. Therefore, we used different probe immobilization methods as adsorption, electrostatic attraction and covalent attachment onto the working electrodes to improve experimental conditions for the interaction of 2-Bip and DNA.

As one probe immobilization technique, adsorption is the simplest technique for DNA immobilization and does not require neither chemical reagents nor complex modification steps. In this technique, probe sequences are immobilized onto the working electrodes via passive adsorption without any specific binding procedure. However, poor reproducibility and low sensitivity are the main problems of this technique. In electrostatic attraction technique, immobilization of DNA probes can be improved and stabilized by applying a positive potential to the electrodes immersed in probe solution.

In covalent attachment technique, DNA probe is typically linked with amine groups (NH_2) at the end of 3′ or 5′ to bind covalently to the electrode surface modified with specific reagents, i.e., NHS and EDC. Unlike adsorption technique, covalent attachment shows better stability, higher binding strength and selectivity.

Figure 4 (A: adsorption, B: electrostatic attraction, C: covalent attachment) shows different probe immobilization methods by measuring signals of 2-Bip and guanine. Decrease rate of 2-Bip and guanine oxidation signals were shown in Table 1.

As shown in the figure, guanine signals of probe were higher than hybrid since the oxidation is more difficult in the closed form (hybrid structure) compared to open one (probe structure). The obstacle in the transfer of electrons from the inside of rigid dsDNA to the electrode surface is much troublesome compared to flexible ssDNA where the bases are in closer proximity to the electrode surface, leading to higher peak currents in ssDNA. Our results demonstrate that complementary target could form a hybrid structure with the probe, resulting in a significant decrease in the magnitude of the guanine signal due to the hybridization. When 2-Bip was interacted with probe and hybrid, the anodic peak current of both 2-Bip and guanine decreased for all methods.

Signal decrease (%) is defined as $(I_{before}-I_{after})/I_{before}) \times 100$, where I_{before} and I_{after} are DPV current signals of 2-Bip and guanine measured before and after the interaction with each other, respectively. An oxidation signal decrease was nearly ~60 % and ~30 % for 2-Bip and guanine, respectively for adsorption method (Figure 4A). Guanine signal decrease was nearly 5.2 % and 8.4 % for probe and hybrid respectively for electrostatic attraction method (Figure 4B) that indicates nearly no interaction presents with DNA and 2-Bip, while 2-Bip signal dramatically decreases (~40 % for probe and ~70 % for hybrid). This is due to the higher accumulated amount of 2-Bip

Table 1. Decrease of 2-Bip and guanine signals obtained from 2-Bip, probe, probe + 2-Bip, hybrid and hybrid + 2-Bip for different probe immobilization methods.

Probe Immobilization Method	2-Bip Oxidation Signal Decrease (%)		Guanine Oxidation Signal Decrease (%)	
	Probe	Hybrid	Probe	Hybrid
Adsorption	62,8	65,3	34,2	31,4
Electrostatic attraction	42,3	77,1	5,2	8,4
Covalent attachment	46,7	39,1	32,6	22,0

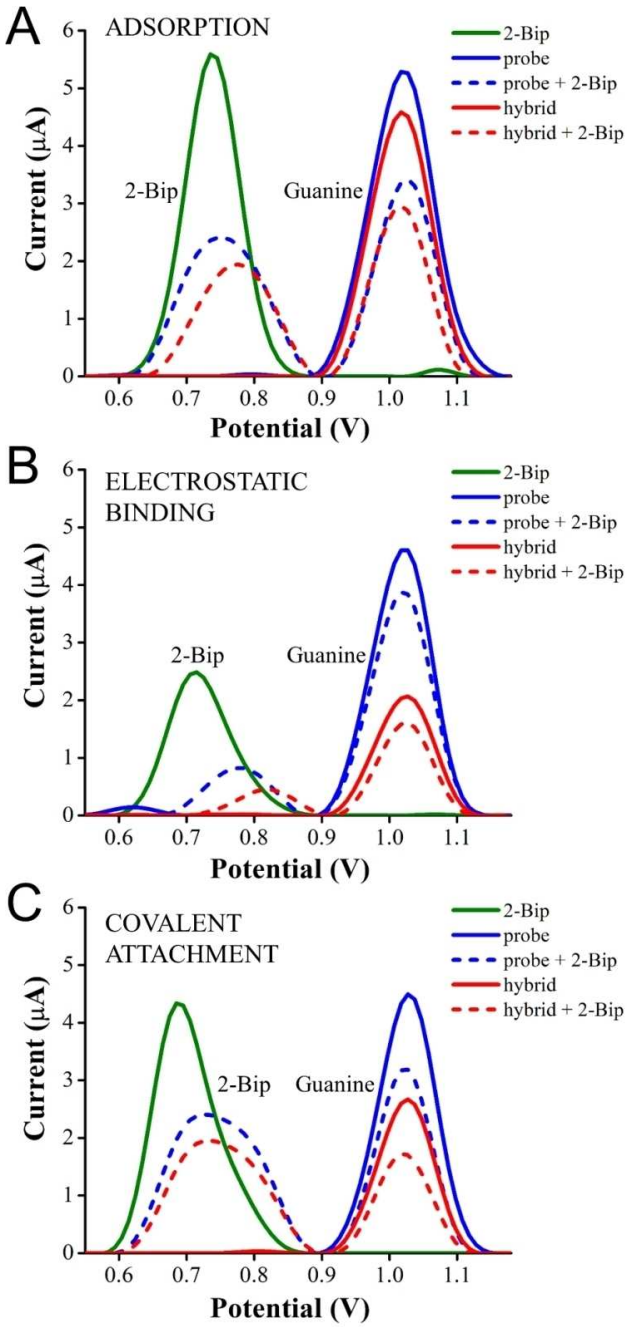

Fig. 4. Voltammogram of oxidation signals of 2-Bip (0.75 V) and guanine (1.0 V) measured for 2-Bip, probe, probe + 2-Bip, hybrid and hybrid + 2-Bip coated PGEs for (**A**) adsorption, (**B**) electrostatic binding and (**C**) covalent attachment methods with DPV. The corresponding experimental procedure: PGEs pretreatment, 5 μg/mL probe immobilization, interaction with 7 μg/mL target for 30 min., rinsing with PBS, interaction with 15 μg/mL 2-Bip for 7 min., and DPV measurement by scanning between 0.55 V and 1.15 V in PBS.

increased the decrease of its oxidation. Higher accumulation of 2-Bip onto electrode is because of less accumulation of DNA onto the electrode surface with electrostatic binding. In covalent attachment (Figure 4C), oxidation signal decrease was nearly ~40 % and ~30 %

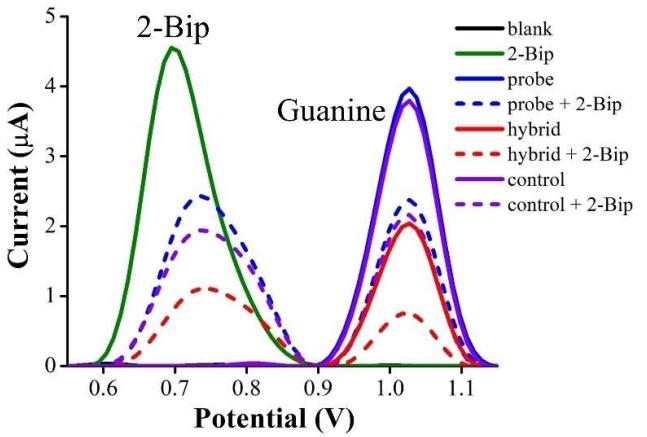

Fig. 5. Voltammogram of oxidation signals of 2-Bip (0.75 V) and guanine (1.0 V) measured for 2-Bip, probe + 2-Bip, hybrid + 2-Bip and control + 2-Bip coated PGEs with DPV under the optimum conditions.

for 2-Bip and guanine, respectively. These results indicated that adsorption technique was more desirable for probe immobilization compared to electrostatic attraction and covalent attachment techniques.

According to these observations, it seems that the decrease of peak current of 2-Bip after interaction with dsDNA is not caused by the intercalation of 2-Bip to the bulk, slowly diffusing dsDNA, which results in considerable decrease in the expected current. However, similar results were obtained with ssDNA that explain the interaction mode can not be intercalation because ssDNA contains only one chain, which does not allow 2-Bip to accumulate into DNA.

In Figure 5, the interaction of 2-Bip with probe, hybrid and control sequences were shown under optimum conditions. Control sequences were also used to determine the selectivity of the constructed biosensor, i.e., probe and control signals were close as they were not hybridized with each other. Current signals of probe, hybrid and control dramatically decreased after the interaction with 2-Bip, while their decreasing amount was different. There was no measurable shift in the oxidation peak potential for guanine upon the interaction with 2-Bip. On the other hand, 2-Bip oxidation signal decreased in amplitude and shifted along the potential axis after the interaction with probe, hybrid and control sequences.

The limit of detection (LOD) was found as 4.2 μmol L^{-1}. The repeatability was calculated from the relative standard deviation (RSD) as 3.4 %, 4.9 %, 6.4 % and 7.6 % for probe, hybrid, control, probe + 2-Bip and hybrid + 2-Bip, respectively (n = 5).

In addition, binding constant (DNA + Small Molecule↔DNA-Small Molecule) was calculated from the equation below [25]:

$$\log\,(1/[\mathrm{DNA}]) = \log K + \log(I_{\mathrm{before}})/(I_{\mathrm{before}} - I_{\mathrm{after}}) \qquad (1)$$

where K is the apparent binding constant, I_{before} is the peak current of the compound before interaction (μA), and I_{after} is the peak current of the compound in the presence of DNA (μA).

In this experiment, concentration of 2-Bip were kept constant while varying the concentration of ssDNA for DPV measurements. According to Equation 1, expected binding constant of 2-Bip to ssDNA was found as 5×10^5, which coincides well with other molecules in literature [3a,26]. For instance, the binding constants of molecules that bound to DNA is between 10^4–10^6 M^{-1}, which is very constituent with our results [27]. The calculated K value indicated that the complexes formed at the physiological pH level were stable such that there was a very strong interaction of 2-Bip with ssDNA and dsDNA. The change in the Gibbs free energy (ΔG°) was calculated since it accounts for the stability of the complexes with the following equation:

$$\Delta G^\circ = -R.T.\ln K \quad (2)$$

Using Equation 2, ΔG° was found as $-32.50\ kJ\,mol^{-1}$. This ΔG° value proved that the interaction process was spontaneous and favorable. Toxicity effect of 2-Bip on DNA was calculated with the following equation [28]:

$$S\% : (S_s/S_b).100 \quad (3)$$

S% refers to the percentage of the guanine peak height change, S_s is the magnitude of the guanine peak after the interaction with sample and S_b is the magnitude of the guanine peak after the interaction with blank solution. S% value was calculated as 60 % for probe and 37 % for hybrid, which means 2-Bip is moderately toxic to ssDNA and toxic to dsDNA (sample with S% > 85 is non-toxic, S% between 50 and 85 is moderately toxic, and S% < 50 is toxic).

In drug-DNA interaction studies, redox properties of drug molecules are investigated since the drug molecules give oxidation or reduction peaks, i.e., it is possible to determine hybridization using these signals that belongs to a drug. Electrochemical based hybridization indicators are widely used to detect DNA hybridization events and usually electroactive compounds with small molecular weight and different affinities for ssDNA and dsDNA. For instance; transition metal complexes, i.e., ligands or cationic metal complexes (Ruthenium (II), Copper (II), Cadmium(II) and Cobalt (II) complexes), have been widely used as electrochemical hybridization indicators or electroactive markers of DNA [29]. Especially, Ruthenium complexes are having great attention for their capability for selective binding DNA through intercalation [30]. Despite their wide usage, these redox metal complexes molecules generally covalently conjugated with polymers for the attachment of metal complexes probes to nucleobases. These additional step could time consuming and requires an extra experimental step. Additionally, Meldola Blue, a widely used DNA hybridization agent, is toxic.

Our findings demonstrate that 2-Bip can be used as a new electrochemical indicator, which is able to detect hybridization of probe and hybrid both via 2-Bip and guanine oxidation signal changes at the same time. Monitoring the hybridization with alternative hybridization indicators such as Meldola's blue, Methylene blue or phenanthroline derivatives is critical for the sequences not containing guanine bases. 2-Bip behaves like a hybridization indicator due to its distinct electrochemical behavior to different strands of DNA.

4 Conclusion

The development of fast and accurate methods for the detection of interaction between potential drug molecules with DNA is extremely important. In this study, a label-free electrochemical method for the detection of 2-Bip and its interaction with ssDNA and dsDNA was developed via a biosensor system with voltammetric techniques. The oxidation signals of 2-Bip and guanine were used to determine the possible interaction of 2-Bip with DNA. The presented voltammetric platform possesses the advantages of short analysis time, low cost and simplicity. DPV also provides lower signal-to-noise ratio compared to steady state techniques. Further investigations such as quantum mechanical calculations for conformational analysis, molecular docking calculations, foot-printing and affinity cleavage and molecular dynamics simulation of 2-Bip with DNA are planned for future developments of the electrochemical sensor platform.

Acknowledgements

S. N. T. acknowledges Izmir Katip Celebi University 2018-GAP-ECZF-0002 Grant.

References

[1] a) S. N. Topkaya, V. H. Ozyurt, A. E. Cetin, S. Otles, *Biosens. Bioelectron.* **2018**, *102*, 464–469; b) S. N. Topkaya, G. Serindere, M. Ozder, *Electroanalysis* **2016**, *28*, 1052–1059.

[2] a) M. Shabbir, I. Ahmad, H. Ismail, S. Ahmed, V. McKee, Z. Akhter, B. Mirza, *Polyhedron* **2017**, *133*, 270–278; b) E. Mirmomtaz, A. Zirakbash, A. A. Ensafi, *Russ. J. Electrochem.* **2016**, *52*, 320–329; c) M. Sirajuddin, S. Ali, A. Badshah, *J. Photochem. Photobiol. B* **2013**, *124*, 1–19; d) J. C. Garcia-Ramos, R. Galindo-Murillo, F. Cortes-Guzman, L. Ruiz-Azuara, *J. Mex. Chem. Soc.* **2013**, *57*, 245–259; e) T. T. Gu, Y. Hasebe, *Biosens. Bioelectron.* **2012**, *33*, 222–227; f) D. L. Ma, D. S. H. Chan, P. Lee, M. H. T. Kwan, C. H. Leung, *Biochimie* **2011**, *93*, 1252–1266.

[3] a) K. Morawska, T. Poplawski, W. Ciesielski, S. Smarzewska, *Bioelectrochemistry* **2018**, *123*, 227–232; b) N. Arshad, S. I. Farooqi, *Appl. Biochem. Biotechnol.* **2018**, *186*, 1090–1110; c) F. Abul Qais, I. Ahmad, *J. Pharm. Biomed* **2018**, *149*, 193–205; d) Y. Rahman, S. Afrin, M. A. Husain, T.

Sarwar, A. Ali, Shamsuzzaman, M. Tabish, *Arch. Biochem. Biophys.* **2017**, *625*, 1–12.
[4] a) A. Mukherjee, S. Mondal, B. Singh, *Int. J. Biol. Macromol.* **2017**, *101*, 527–535; b) H. S. Haniff, A. Graves, M. D. Disney, *ACS Comb. Sci.* **2018**, *20*, 482–491; c) S. E. Seo, M. X. Wang, C. M. Shade, J. L. Rouge, K. A. Brown, C. A. Mirkin, *ACS Nano* **2016**, *10*, 1771–1779; d) Y. K. Jung, H. G. Park, *Biosens. Bioelectron.* **2015**, *72*, 127–132.
[5] a) S. Vembanur, K. Halvorsen, C. Myers, A. Chen, M. Yigit, *Biophys. J.* **2015**, *108*, 231a–232a; b) M. Monajjemi, F. Mollaamin, *J. Cluster Sci.* **2012**, *23*, 259–272.
[6] T. Ellis, D. A. Evans, C. R. H. Martin, J. A. Hartley, *Nucleic Acids Res* **2007**, *35*.
[7] S. Dogra, P. Awasthi, S. Tripathi, T. P. Pradeep, M. S. Nair, R. Barthwal, *J. Biomol. Struct. Dyn.* **2014**, *32*, 1164–1183.
[8] M. Raja, J. Alberti, J. Saurina, S. Sentellas, *Anal. Bioanal. Chem.* **2016**, *408*, 3911–3922.
[9] C. J. Baltazar, R. Mun, H. A. Tajmir-Riahi, J. Bariyanga, *J. Mol. Struct.* **2018**, *1161*, 273–278.
[10] M. Torres, S. Khan, N. Mirsaleh-Kohan, *Abstr Pap Am Chem S* **2015**, *250*.
[11] F. Araya, G. Huchet, L. McGroarty, G. G. Skellern, R. D. Waigh, *Methods* **2007**, *42*, 141–149.
[12] F. C. Loo, S. P. Ng, C. M. L. Wu, S. K. Kong, *Sens. Actuators B-Chem* **2014**, *198*, 416–423.
[13] M. A. Husain, H. M. Ishqi, T. Sarwar, S. U. Rehman, M. Tabish, *MedChemComm* **2017**, *8*, 1283–1296.
[14] a) A. Borowik, R. Banasiuk, N. Derewonko, M. Rychlowski, M. Krychowiak-Masnicka, D. Wyrzykowski, M. Ziabka, A. Woziwodzka, A. Krolicka, J. Piosik, *Sci Rep-Uk* **2019**, *9*; b) Y. You, K. Zhou, B. Y. Guo, Q. S. Liu, Z. Cao, L. Liu, H. C. Wu, *ACS Sens.* **2019**, *4*, 774–779; c) D. Inci, A. Koseler, A. Zeytunluoglu, R. Aydin, Y. Zorlu, *J. Mol. Struct.* **2019**, *1177*, 317–322.
[15] Y. Zhang, J. Hu, C. Y. Zhang, *Anal. Chem.* **2012**, *84*, 9544–9549.
[16] a) J. Wang, Y. F. Li, C. Li, X. P. Zeng, W. W. Tang, X. J. Chen, *Microchim. Acta* **2017**, *184*, 2999–3006; b) H. Ilkhani, T. Hughes, J. Li, C. J. Zhong, M. Hepel, *Biosens. Bioelectron.* **2016**, *80*, 257–264.
[17] A. A. El Rashedy, H. Y. Aboul-Enein, *Mini-Rev. Med. Chem.* **2013**, *13*, 399–407.
[18] a) N. O. Anastassova, D. Y. Yancheva, A. T. Mavrova, M. S. Kondeva-Burdina, V. I. Tzankova, N. G. Hristova-Avakumova, V. A. Hadjimitova, *J. Mol. Struct.* **2018**, *1165*, 162–176; b) A. Bergamo, P. J. Dyson, G. Sava, *Coord. Chem. Rev.* **2018**, *360*, 17–33; c) A. A. Farahat, M. A. Ismail, A. Kumar, T. Wenzler, R. Brun, A. Paul, W. D. Wilson, D. W. Boykin, *Eur. J. Med. Chem.* **2018**, *143*, 1590–1596; d) T. Vausselin, K. Seron, M. Lavie, A. A. Mesalam, M. Lemasson, S. Belouzard, L. Feneant, A. Danneels, Y. Rouille, L. Cocquerel, L. Foquet, A. R. Rosenberg, C. Wychowski, P. Meuleman, P. Melnyk, J. Dubuisson, *J. Virol.* **2016**, *90*, 8422–8434; e) X. F. Han, X. He, M. Wang, D. Xu, L. P. Hao, A. H. Liang, J. Zhang, Z. M. Zhou, *Eur. J. Med. Chem.* **2015**, *103*, 473–487.
[19] a) C. Karaaslan, F. Bakar, H. Goker, *Z. Naturforsch. C* **2018**, *73*, 137–145; b) A. Gangrade, V. Pathak, C. E. Augelli-Szafran, H. X. Wei, P. Oliver, M. Suto, D. J. Buchsbaum, *Int J Mol Sci* **2018**, *19*; c) J. E. Cheong, M. Zaffagni, I. Chung, Y. J. Xu, Y. Q. Wang, F. E. Jernigan, B. R. Zetter, L. J. Sun, *Eur. J. Med. Chem.* **2018**, *144*, 372–385.
[20] H. M. Refaat, *Eur. J. Med. Chem.* **2010**, *45*, 2949–2956.
[21] H. T. Abdel-Mohsen, F. A. F. Ragab, M. M. Ramla, H. I. El Diwani, *Eur. J. Med. Chem.* **2010**, *45*, 2336–2344.
[22] M. Shaharyar, M. M. Abdullah, M. A. Bakht, J. Majeed, *Eur. J. Med. Chem.* **2010**, *45*, 114–119.
[23] Y. Luo, F. Xiao, S. J. Qian, W. Lu, B. Yang, *Eur. J. Med. Chem.* **2011**, *46*, 417–422.
[24] a) S. N. Topkaya, *Biosens. Bioelectron.* **2015**, *64*, 456–461; b) V. Ratautaite, S. N. Topkaya, L. Mikoliunaite, M. Ozsoz, Y. Oztekin, A. Ramanaviciene, A. Ramanavicius, *Electroanalysis* **2013**, *25*, 1169–1177; c) T. Kilic, S. N. Topkaya, D. O. Ariksoysal, M. Ozsoz, P. Ballar, Y. Erac, O. Gozen, *Biosens. Bioelectron.* **2012**, *38*, 195–201; d) S. N. Topkaya, S. Aydinlik, N. Aladag, M. Ozsoz, D. Ozkan-Ariksoysal, *Comb. Chem. High Throughput Screening* **2010**, *13*, 582–589.
[25] Q. Feng, N. Q. Li, Y. Y. Jiang, *Anal. Chim. Acta* **1997**, *344*, 97–104.
[26] a) M. Dribek, I. Le Potier, A. Rodrigues, A. Pallandre, E. Fattal, M. Taverna, *Electrophoresis* **2007**, *28*, 2191–2200; b) K. Lozano, F. D. Ferreira, E. G. da Silva, R. C. dos Santos, M. O. F. Goulart, S. T. Souza, E. J. S. Fonseca, C. Yanez, P. Sierra-Rosales, F. C. de Abreu, *J. Solid State Electrochem.* **2018**, *22*, 1483–1493; c) B. Rafique, A. M. Khalid, K. Akhtar, A. Jabbar, *Biosens. Bioelectron.* **2013**, *44*, 21–26.
[27] S. Nafisi, A. A. Saboury, N. Keramat, J. F. Neault, H. A. Tajmir-Riahi, *J. Mol. Struct.* **2007**, *827*, 35–43.
[28] G. Bagni, D. Osella, E. Sturchio, M. Mascini, *Anal. Chim. Acta* **2006**, *573–574*, 81–89.
[29] a) M. Fojta, L. Havran, H. Pivonkova, P. Horakova, M. Hocek, *Curr. Org. Chem.* **2011**, *15*, 2936–2949; b) F. Li, W. Chen, C. F. Tang, S. S. Zhang, *Talanta* **2008**, *77*, 1–8.
[30] a) W. Q. Bai, Y. Y. Wei, Y. C. Zhang, L. Bao, Y. Li, *Anal. Chim. Acta* **2019**, *1061*, 101–109; b) T. Garcia-Mendiola, T. B. Martinez, F. Pariente, J. Molano, E. Lorenzo, *Electroanalysis* **2014**, *26*, 1362–1372; c) S. W. Dutse, N. A. Yusof, H. Ahmad, M. Z. Hussein, Z. Zainal, *Int. J. Electrochem. Sci.* **2012**, *7*, 8105–8115.

Received: March 25, 2019
Accepted: April 22, 2019
Published online on ■■, ■■

FULL PAPER

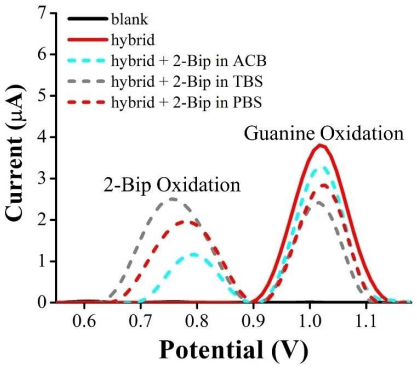

S. N. Topkaya, A. E. Cetin*